



Research Article

## Thermodynamic sensitivity analysis of SOFC integrated with blade cooled gas turbine hybrid cycle

Tushar CHOUDHARY<sup>1</sup>, Tikendra Nath VERMA<sup>2,\*</sup>, Mithilesh Kumar SAHU<sup>3</sup>,  
Upendra RAJAK<sup>4</sup>, SANJAY<sup>5</sup>

<sup>1</sup>Department of Mechanical Engineering, PDPM Indian Institute of Information Technology, Design and Manufacturing, Jabalpur, M.P, 482005, India

<sup>2</sup>Department of Mechanical Engineering, Maulana Azad National Institute of Technology Bhopal, M.P, 462003, India

<sup>3</sup>Department of Mechanical Engineering, OP Jindal University Raigarh, C.G, 496109, India

<sup>4</sup>Department of Mechanical Engineering, RGM College of Engineering and Technology, Nandyal, A.P, 496109, India

<sup>5</sup>Department of Mechanical Engineering, National Institute of Technology Jamshedpur, Jharkhand, 83101 India

### ARTICLE INFO

#### Article history

Received: 2 March 2021

Accepted: 24 June 2021

#### Keywords:

SOFC; Hybrid Cycle;

Gas Turbine; Efficiency

### ABSTRACT

In the area of clean energy production along with higher efficiency, integrated combine power system, specifically gas turbine (GT) cycle with solid oxide fuel (SOFC) system, is gaining the attention of researchers. Thermodynamic modeling for the SOFC-GT hybrid cycle has been presented in this paper. For the proposed hybrid cycle, a high-temperature SOFC has successfully integrated with the recuperated-blade cooled gas turbine cycle. The gas turbine outlet waste heat has perfectly utilized the recuperator to power the fuel cell system. However, to maintain the temperature of the gas turbine blade within the permissible limit, air–film blade cooling scheme has been used. The SOFC-GT hybrid cycle has been operated under steady-state conditions, and a developed MATLAB program has been used to solve the governing equations for the components of the hybrid cycle. The impact of main operating parameters such as the temperature intake turbine (TIT), compression ratio ( $r_{pc}$ ), fuel utilization ratio ( $U_p$ ), and recirculation ratio are examined. From the obtained result, it can be revealed that the integration of the SOFC has seen significant improves overall hybrid cycle efficiency. The performance of fuel cell (SOFC) increases notably as the level of recuperation increases. To check the influence of main operating parameters, a sensitivity analysis has been performed for the hybrid cycle, and the maximum efficiency of 73% has been achieved. Moreover, to extend this research, an exclusive performance map has been plotted for power plant designers.

**Cite this article as:** Choudhary T, Verma TN, Sahu MK, Rajak U, Sanjay Thermodynamic sensitivity analysis of SOFC integrated with blade cooled gas turbine hybrid cycle. J Ther Eng 2023;9(1):205–217.

\*Corresponding author.

\*E-mail address: [verma.tikks@gmail.com](mailto:verma.tikks@gmail.com)

This paper was recommended for publication in revised form by Regional Editor

Nader Javani



## INTRODUCTION

The primary objective of the research is to develop some novel energy conversion technologies in the field of energy and power generation with higher efficiencies and lower environmental impacts. Due to drastic development in emerging countries, the energy sector has faced a continuous increase in world energy consumption. Therefore, it is essential to make such development “sustainable,” considering the limited availability of natural resources.[1]

To generate power for domestic, electrical utility, automotive, industrial, and commercial sectors, fuel cell is regarded as one of the future promising power generation means that offer nearly zero-emission, flexible fuel utilization, and efficient energy conversion rates. Solid oxide fuel cell (SOFC) is known to be a potential alternative for clean power production. In SOFC, direct energy conversion takes place, i.e., electrochemical reaction to electrical energy; therefore, it is not subjected to limitations of Carnot engine. In regard to exergy loss, in SOFC the exergy losses associated during oxidation of fuel is comparatively very low in comparison with the conventional combustion of fuel.

Unlike other low operating temperature fuel cells, SOFC operates at a high temperature, thus facilitating internal reforming of fuel. Hydrogen is produced during internal reforming, which reacts electrochemically and generates both electric power and high-grade waste heat used for the combined heat and power (CHP) system.

Simulation has already demonstrated SOFC can achieve a net electrical performance of more than 60 percent and is known to be the most practical approach to achieve a considerably high electrical efficiency in effective integration of multi-MW gas turbine engines[2]. In 1987 Tokyo Gas and Westinghouse jointly placed the first milestone in the evolution of SOFC power generation systems and developed some applications for SOFC. In 2000 Siemens-Westinghouse Power Corporation developed the first pressurized SOFC-GT power system by integrating the gas turbine engine with the SOFC stack. The energy efficiency of the installed unit is 55% and produces 220 kW of electricity. [3].

In recent years, numerous studies into the SOFC-GT hybrid power cycle have been reported to explore various aspects of the technology for hybrid energy conversion. Fredriksson et al. [4] have performed optimization of SOFC-GT system along with carbon-capturing system using genetic algorithm. Their key aim is to simplify the multi-variable non-linear SOFC-GT cycle problem. Song et al. [5] analyzed the efficiency characteristics of SOFC-GT hybrid cycle SOFC-GT component load operations and proposed to boost performance degradation by retaining the same turbine and fuel cell operating temperature. Akkaya et al. [6] have performed exergy analysis for SOFC/GT CHP-based system. A new performance parameter has been used to judge the system's exergy in terms based on

the exergetic performance coefficient. Rambabu et al.[7] defined a dynamic SOFC lumped model and provided the control strategy for the self-contained SOFC-GT system developed. Santinetal.[8] conducted thermo-economic research for 500 kW SOFC-GT hybrid device powered by liquid fuels. In their work, they have compared four different configurations of SOFC-GT cycle. They found that methanol fuelled system has maximum hybrid efficiency as compared to kerosene one. To maximize the overall efficiency, Adams et al. [9] proposed a flexible polygeneration plant where SOFC has been integrated to produce fuel and electricity. They also conclude that the heating value, feed rate, and composition play a significant role in power generation. For achieving higher efficiency up to 80%, along with additional power, can be attained by integrating SOFC thermally or chemically with bottoming cycles, such as Brayton, Rankine[10], Kalina[11], Stirling cycles[12], tri-generation system[13], CHP application[14], APU system[15] and storage devices along with renewable has been renewable energy conversion systems[16].

Besides these typical integrations of SOFC with GT and other power generation systems, several researchers focused on computational and numerical modeling, such as Choudhary et al. [17-19], Fragiaco [20], Peksen et al.[21] and He et al. [22]

Zhao et al. [28] proposed a novel integration between SOFC and chemical looping hydrogen generation. The key aspect of their integration is that it generates power, separates, and captures carbon dioxide without power consumption. The proposed system has energy and exergy efficiency of 65% and 60%, respectively.

Hayri et al. [29] develop a three-dimensional model to predict the degradation level of planar SOFC when fueled with coal syn-gas. The developed model has been calibrated with the experimental work. The results show how the degradation level impacts the current and temperature distribution throughout the cell.

Akroot et al. [30] compare the performance of two SOFC-GT hybrid systems. In their work, two different SOFC models have been used; the models used are anode supported model and electrolyte supported model. They chiefly examine the impact of fuel cell operating temperature and steam to carbon ratio. From the comparison, anode supported model has superior performance as compared to electrolyte supported model. The anode-supported model yields a power of 695kW and has an efficiency of 64.6%. Furthermore, they also concluded that lower steam to carbon ratio favors fuel cell power output and results in high efficiency.

Guo et al.[31] conducted the performance analysis for SOFC integrated with the turbo-fan engine for UAV applications. As a novelty, Al-H<sub>2</sub>O reactor system has been coupled with the entire system for flight power generation. In comparison to turbo-fan engines, the integrated system decreases fuel consumption by more than 10%.

From the comprehensive literature review, it has been found that no such work has been reported where a cooled gas turbine engine has been integrated with internal reformed SOFC. In contrast, the research related to gas turbine cooling exhibits [23-26] and is still in maturing stage.

This article aims to successfully integrate the high-temperature fuel cell (SOFC) with a novel gas turbine model (blade cooled gas turbine). For this, a detailed, comprehensive thermodynamic model has been discussed in detail. The integration includes the recuperated-blade cooled gas turbine cycle was incorporated thermally in the internally reformed high-temperature SOFC. The established MATLAB software analyzed the effect of various output parameters such as turbine intake temperature, pressure ratio, fuel consumption ratio, recirculation under steady-state conditions. In addition, a sensitivity study was conducted where the effect of operational parameters on efficiency parameters was addressed in depth.

**SYSTEM DESCRIPTION**

The scheme of the hybrid cycle SOFC-GT is explained in Fig.1. The proposed SOFC-GT hybrid cycle contains six elements, e.g., pump, compressor, recuperator, combustion chamber, fuel cell (SOFC), and gas turbine. To power up the hybrid cycle, sys-gas has been used. Here the working fluid is air, and its behavior in terms of temperature, enthalpy, and enthalpy is examined in fig. 2. At state 1 the air enters the compressor and gets pressurized; the pressurized air enters the recuperator and gets preheated before entering the fuel cell. However, the recuperator has been charged by utilizing the high grade of available waste heat at the gas turbine outlet. Consequently, the performance of the hybrid cycle can be improved by the recuperation process. In a fuel cell, pressurized fuel and air enter at the same temperature at the cathode and anode channel, where an electrochemical reaction occurs, and reaction specifics are described in the modeling section of fuel cells. The fuel cell bi-product consists of unused syn-gas, heat, and electricity

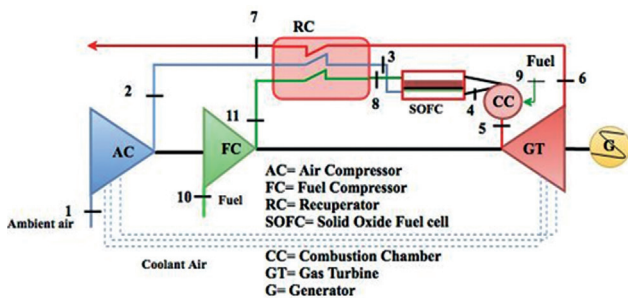


**Figure 1.** SOFC-GT (blade cooled gas turbine) hybrid cycle schematic configuration.

(DC). In the combustion chamber, the unutilized syn-gas is completely burnt to reach desired turbine inlet temperature (TIT). In the gas turbine, the blades of a turbine are exposed to high temperature and flue gasses strain, resulting in critically high-temperature oxidation and creeping blade failure. Therefore, the air/blade cooling system was used to maintain the temperature of the gas turbine blade within the permitted limit. The compressed air was bled from the compressor at various times in order to cool the turbine blade. Though the working fluid has enough potential and is allowed to expand within the gas turbine to generate use full work. The operating parameters of SOFC and Gas turbine has been referred from the work of Sanjay [23] and Colpan [32].

**Modelling and Simulation**

SOFC-GT hybrid cycle thermodynamic analysis has been conducted with the aid of solving the cycle part equation. Table 1 provides the hybrid cycle parameters and operational parameters used to calculate thermodynamic properties at multiple cycle stages (pressure, temperature and enthalpy). The thermodynamic modeling of the cycle components for the acquisition of all cycle state point properties is as follows:

$$h = \int_{T_a}^T C_p(T) dT \tag{1}$$

$$\varnothing = \int_{T_a}^T C_p(T) \frac{dT}{T} \tag{2}$$

$$s = \varnothing - R \cdot \ln \left| \frac{P}{P_a} \right| \tag{3}$$

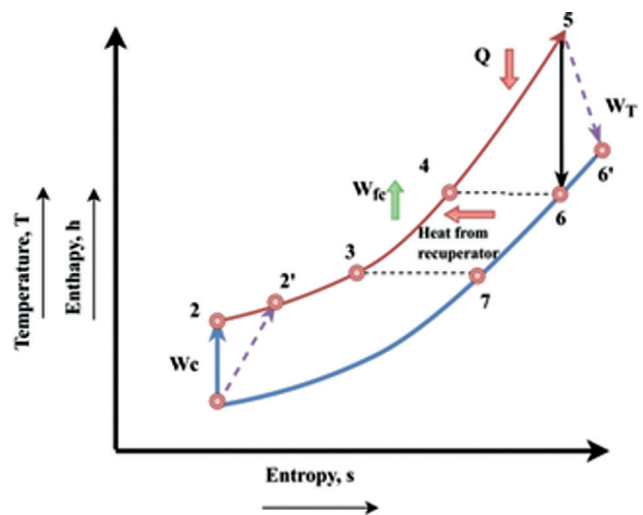


**Figure 2.** SOFC-GT hybrid cycle T-s diagram.

### Compressor

In this work, the isentropic compressor has been considered. The blade-cooled gas turbine model has been used for the hybrid power cycle shown. Coolant (air) is bled from the compressor at an appropriate pressure level to cool the gas turbine blades to avoid the backflow in the gas turbine unit, as shown in Fig 1. Efficiency is as follows in the governing equations for state point and compressor work [23,25]:

$$\eta_{comp} = \frac{W_{comp,ideal}}{W_{comp,actual}} = \frac{h_2 - h_1}{h_2' - h_1} \quad (4)$$

$$\frac{T_2}{T_1} = \left( \frac{P_2}{P_1} \right)^{\left( \frac{\gamma-1}{\gamma} \right)} \quad (5)$$

$$-\dot{W}_{comp} = -\dot{m}_e \cdot h_e + \sum \dot{m}_{c,j} \cdot h_{c,j} - \dot{m}_{c,j} \cdot h_{c,in} \quad (6)$$

### Recuperator

Using recuperator, the available waste heat at the gas turbine outlet has been utilized to charge up the working fluid and fuel. The effectiveness ( $\epsilon$ ) of recuperator is given as [24]:

$$\epsilon = \frac{(T_{rc,a})_e - (T_{rc,a})_{in}}{(T_{rc,g})_{in} - (T_{rc,a})_e} \quad (7)$$

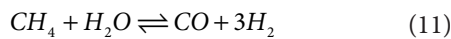
The mass and energy balance equation for the recuperator is expressed as:

$$\dot{m}_{rc,g} \cdot c_{pg} \cdot \psi(T_{g,in} - T_{g,e}) = \dot{m}_{rc,a} \cdot c_{pa} \cdot \psi(T_{g,in} - T_{g,e}) \quad (8)$$

### Fuel Cell (SOFC)

To develop the SOFC-GT hybrid system, high-temperature internal reformed SOFC has been integrated, fueled by syn-gas. The following main assumptions were considered in the SOFC model: equilibrium reforming and shifting reactions; adiabatic cell; anode-cathode exit streams of equal temperature; cathode channel composed of  $O_2$  and  $N_2$ ; electrical flow-responsible  $H_2$  ion transport; and anode channel composed of  $CO$ ,  $CO_2$ ,  $CH_4$ ,  $H_2$ ,  $H_2O$ ; flow-stream pressure decrease of 3%.

The electrochemical reactions inside the fuel cell anode and cathode are as follows :



Overall Fuel Cell Reaction:



The general solutions for the conservation of fuel cell mass and energy equations include the calculation of the voltage and current produced in the cell. The polarization (loss) inside the SOFC is induced by three sources: activation polarization (Vact), ohms (Vohm), and concentration polarization (Vconc). Different governing equations are used to measure the individual output characteristics of SOFC Eq. [14-22]. In Choudhary et al. [17, 18, and 27] the full procedures for computing cell voltage and loss were detailed.

$$E_{Nernst} = \frac{\Delta G_T^0}{n_e F} + \frac{RT}{n_e F} \ln \left( \frac{X_{H_2} X_{O_2}^{0.5}}{X_{H_2O}} \right) + \frac{1}{2} \frac{RT}{n_e F} \ln \left( \frac{P}{P^0} \right) \quad (14)$$

$E_{Nernst}$  Varies from 0.99 V-1.01V.[29].

Activation Polarization:

$$E_{act} E_{act,a} + E_{act,c} = \frac{RT}{F} \cdot \sin^{-1} \left( \frac{i}{2i_{cd,a}} \right) + \frac{RT}{F} \cdot \sin^{-1} \left( \frac{i}{2i_{cd,c}} \right) \quad (15)$$

Ohmic polarization:

$$E_{ohm} = R_{ohm} \cdot i = \left( \frac{\tau_a}{\sigma_a} + \frac{\tau_{elec}}{\sigma_{elec}} + \frac{\tau_c}{\sigma_c} \right) = (R_{contact} + \sum_k \rho_k \cdot L_k) i \quad (16)$$

Concentration Polarization:

$$E_{conc} = E_{conc}^a + E_{conc}^c = \left[ \frac{-RT}{n_e F} \ln \left( 1 - \frac{i}{i_{as}} \right) + \frac{RT}{n_e F} \ln \left( 1 + \frac{X_{H_2}}{X_{H_2O}} \frac{i}{i_{as}} \cdot \frac{P}{P^0} \right) \right] + \left[ \frac{-RT}{n_e F} \ln \left( 1 - \frac{i}{i_{cs}} \right) \right] \quad (17)$$

Where,

$$i_{as} = \frac{n_e F \cdot X_{H_2} \cdot D_{ceff} \cdot P}{RT \cdot \tau_a} \quad (17a)$$

$$i_{cs} = \frac{n_e F \cdot X_{O_2} \cdot D_{ceff} \cdot P}{\left( 1 - \frac{X_{O_2} P}{X_{O_2} P^0} \right) RT \cdot \tau_a} \quad (17b)$$

SOFC's actual cell voltage is calculated by eq.[27,30] .:

$$E = E_{Nernst} - E_{act} - E_{ohm} - E_{conc} \quad (18)$$

The current produced in the fuel cell is given as:

$$I = i \cdot A = 2F \cdot c = \frac{\dot{m}_f^{H_2}}{1 - r + r \cdot U_F} \quad (19)$$

In this case,  $r$  is called the recirculation ratio, which helps maintain the steam to carbon ratio of fuel entering the fuel channel to prevent carbon deposition insides the cell.

$$r = \frac{\dot{n}_{fuel,utilised}}{\dot{n}_{fuel,inlet}} \quad (20a)$$

$U_F$  is the fuel consumption ratio, which is the ratio of the quantity of hydrogen reacting electrochemically with the inlet of hydrogen.

$$U_F = \frac{\dot{n}_{H_2,utilised}}{\dot{n}_{H_2,inlet}} \quad (20b)$$

The work produced in the fuel cell is computed by:

$$\dot{W}_{fc} = I \cdot E = I \cdot E \quad (21)$$

Finally, the electrical efficiency ( $\eta_{cell}$ ) of the cell stack is given by eq. as under [31]

$$\eta_{cell} = \bar{n} \cdot \frac{\dot{W}_{fc}}{\dot{m}_f \cdot LHV} \quad (22)$$

### Blade Cooled Gas Turbine

Inside the gas turbine rotor, the products of combustion can expand. If it is not cooled, the temperature of flue gases is very high, resulting in blade material failure due to high-temperature oxidation and creep. Thus, different cooling methods are used to control the temperature of turbine blades within the allowable limits[23]. Air-film cooling technique has been used in this work (Fig. 3). The blade surface temperature must be lower compared to the temperature of the blade material ( $T_b = 1123K$ ) for turbine blade cooling. The governing equations are expressed as:

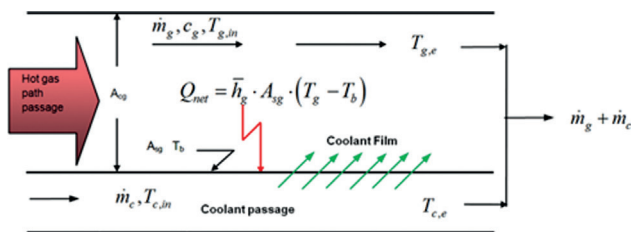


Figure 3. Air film cooling model.

The coolant air mass flow rate ( $\zeta$ ) is given by [23, 24]:

$$\zeta = \frac{\dot{m}_c}{\dot{m}_g} = (1 - \eta_{iso,air}) \cdot \frac{St_{in} \cdot S_g}{\epsilon_c \cdot t \cdot \cos \alpha} \times \frac{c_{pg}(T_{g,in} - T_b)}{c_{p,c}(T_b - T_{c,in})} \times F_{sa} \quad (23)$$

$$\dot{W}_{gt} = \sum_{row} \dot{m}_{g,in} \cdot (h_{g,a_1} - h_{g,b_1})_{cooled} + \sum_{row} \dot{m}_{g,in} \cdot (h_{g,in} - h_{g,e})_{uncooled} \quad (24)$$

$$\eta_{hybrid} = \frac{\dot{W}_{plant}}{\dot{Q}_{total}} \quad (25)$$

$$\dot{W}_{plant} = (\dot{W}_{fc,ac} + \dot{W}_{gt,net}) \cdot \eta_{gen} \quad (26)$$

$$\dot{W}_{gt,net} = \dot{W}_{gt} - \frac{|\dot{W}_{comp}|}{\eta_{mech}} \quad (27)$$

$$\dot{W}_{fc,ac} = W_{fc} \cdot \eta_{invert} \quad \dot{W}_{fc,ac} = W_{fc} \cdot \eta_{invert} \quad (28)$$

$$\dot{Q}_{total} = \dot{m}_{fuel,fc} \times U_F \times LHV_{syn-gas} + Q_{comb} \quad (29)$$

### Combustion Chamber

The products from the fuel cell, i.e. unreacted fuel, air, steam, and operating cycle fluids, are further heated inside the combustion chamber to reach the required turbine inlet temperatures.

The balance of mass and energy in the combustion chamber can be expressed as [24,28]

$$m_f \cdot LHV \cdot \eta_{comb} = m_{comb,e} h_{comb,e} - m_{comb,e} h_{comb,e} \quad (30)$$

$$(\dot{m}_5 + \dot{m}_{fuel,FC} \cdot U_F) h_6 + Q_{comb} = \dot{m}_7 h_7 + \dot{Q}_{loss} \quad (31)$$

$$\dot{Q}_{comb} = [\dot{m}_{fuel,FC} \times (1 - U_F) + \dot{m}_{fuel,comb}] \times LHV \quad (31a)$$

$$\dot{Q}_{loss} = [\dot{m}_{fuel,FC} \times (1 - U_F) + \dot{m}_{fuel,comb}] \times (1 - \eta_{comb}) \times LHV \quad (31b)$$

## RESULT AND DISCUSSION

### Validation

A MATLAB code was developed for each component, based on the thermodynamic modeling as discussed, to simulate SOFC-GT hybrid cycle thermodynamic efficiency characteristics. In order to validate the performance of the integrated SOFC, and standalone SOFC performance has been compared with Massardo and Lubelli et al.[2], Colpan et al.[32] and Tao et al.[33], have validated its performance with previously documented work. The details of validation of SOFC are tabulated in table 2 and table 3.

**Table 1.** Main operating parameters of the SOFC-GT hybrid plant [24, 26, and 27]

Parameters	Values
Compressor Efficiency, $\eta_{comp}$	92%
Turbine efficiency, $\eta_{GT}$	92%
Power turbine efficiency, $\eta_{PT}$	89%
Recuperator effectiveness, $\epsilon$	80%
Combustor efficiency, $\eta_{comb}$	99.5%
Mechanical efficiency, $\eta_{gen}$	98.5%
Alternator efficiency	98.5%
Air inlet temperature,	288K
<b>SOFC parameters</b>	
Wall Condition	Adiabatic
Fuel used	Syn Gas
Composition :Syn Gas { $H_2=40$ , $CH_4=21$ , $CO=20$ , $CO_2=18$ , $N_2=1$ }	%
Air composition : { $N_2=79$ , $O_2 = 21$ }	%
Active surface area (A)	10000mm <sup>2</sup>
Fuel utilization ratio ( $U_F$ )	0.85
Exchange current density of anode ( $i_{cd,a}$ )	0.65A/cm <sup>2</sup>
Exchange current density of cathode ( $i_{cd,c}$ )	0.25A/cm <sup>2</sup>
Effective gaseous diffusivity through the anode ( $D_{a,eff}$ )	0.2cm <sup>2</sup> /s
Effective gaseous diffusivity through the cathode ( $D_{c,eff}$ )	0.05 cm <sup>2</sup> /s
Thickness of anode ( $\tau_a$ )	500 $\mu$ m
Thickness of electrolyte ( $\tau_e$ )	10 $\mu$ m
Thickness of cathode ( $\tau_c$ )	50 $\mu$ m
Electrolyte thermal conductivity	2 W/mK
<b>Pressure Losses</b>	
Compressor inlet plenum loss = 0.5% of entry pressure	
Recuperator and Intercooler gas/air side	1%
Gasturbine exhaust hood loss	1%
Fuel cell Stack	3%
Afterburner	5%

A MATLAB code has been built based on the modeling and governing equation described in previous sections, and the results obtained for the input parameters detailed in Table 1 have been plotted as meaningful graphs. The SOFC model was run, and the results for SOFC handling syn-gas (a mixture of different gases  $CH_4$ ,  $CO_2$ ,  $CO$ ,  $H_2$ , &  $N_2$ ) were obtained with an error of 8.5 percent in contrast to experimental results of Tao et.al. [33] (where pure  $CH_4$  was used), and thus a more significant error.

The fuel cell model was run with pure  $CH_4$  as the fuel to verify the established model with the experimental results of Tao et al. [33] (where pure  $CH_4$  was used), and the simulation results show an error of less than 3.1 percent. Furthermore, the findings have been cross-validated with work by Colpan et al.[32] (using syn-gas), and the error is within 2.1 percent, which is acceptable. The validation of the SOFC model is depicted in Table 3.

Fig 4 shows the pattern of blade coolant mass requirements at various compression ratios and inlet temperature of the turbine. It has shown that the need for blade coolant increases as the TIT and compression ratio increase. It can be inferred from the graph that the variation of TIT on the requirement for blade coolant is more remarkable compared to the variation of the compression ratio. When TIT increases, the heat content within the cycle also increases, and the energy present within the cycle gets available as a useful work through gas turbine expansion. However, the primary challenge is to safeguard the turbine operations, as the turbine blade experiences high thermal stress. Therefore a significant amount of air has been bled from the compressor to maintain the gas turbine blade temperature.

Fig. 5(a) reveals the SOFC-GT Hybrid Cycle Sensitivity Analysis. The influence of change in compression ratio ( $r_{pc}$ ) on thermodynamic performance has been analyzed. The result shows that there is a decrease in gas turbine specific work and turbine efficiency by 0.139% and 0.041, respectively, when  $r_{pc}$  increases from 19 to 20. Whereas, decrease in  $r_{pc}$  from 19 to 18, SOFC efficiency, hybrid efficiency, and hybrid net specific work increases by 0.134%, 0.33%, and 6.29%, respectively.

**Table 2.** Comparison with current uncooled SOFC-GT and the Massardo and Lubelli et al. [2]

Result of Parameters	Massardo and Lubelli et al. [2].	Present SOFC-GT hybrid cycle	Variation
Plant efficiency, %	72.56%, at $r_{pc}$ 20	73.46%, at $r_{pc}$ 20	+1.24%
Hybrid Plant specific work	1700 kJ/kg, at $r_{pc}$ 20	1839 kJ/kg at $r_{pc}$ 20	+8.176%
Power generated by GT, %	37%	33%	-10.81%
Power generated by SOFC, %	63%	67%	6.349%

Table 3. Summary of validation of SOFC performance characteristics

Description of validation	Fuel Used	Error
Proposed model vs. Experimental result of Tao et al. [33]	Syn gas vs. CH <sub>4</sub>	±8.5%
Proposed model vs. Experimental result of Tao et al. [33]	Pure Methane for both	±3.1%
Proposed model vs. Colpan et al.[32]	Syn gas for both	±2.1%

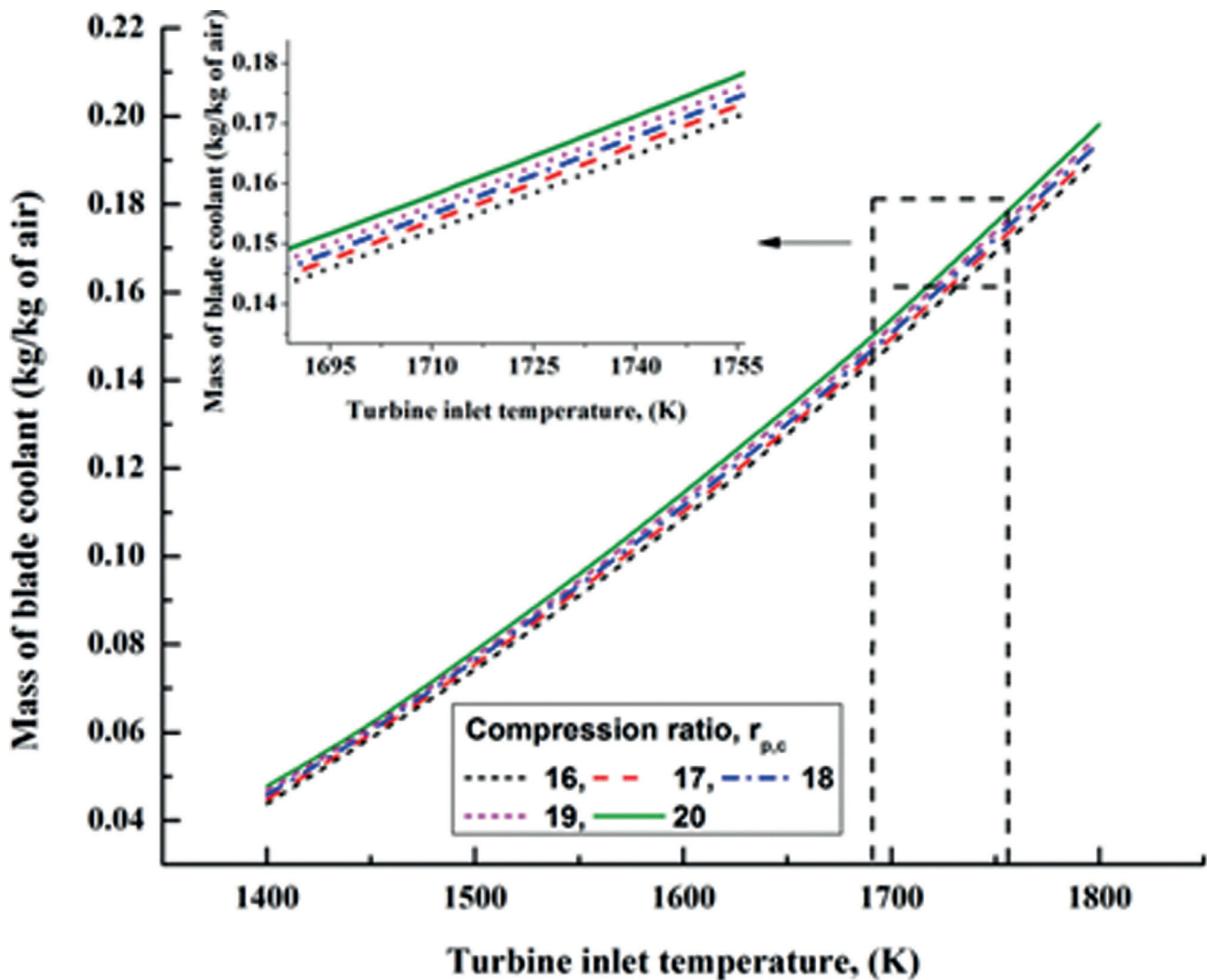
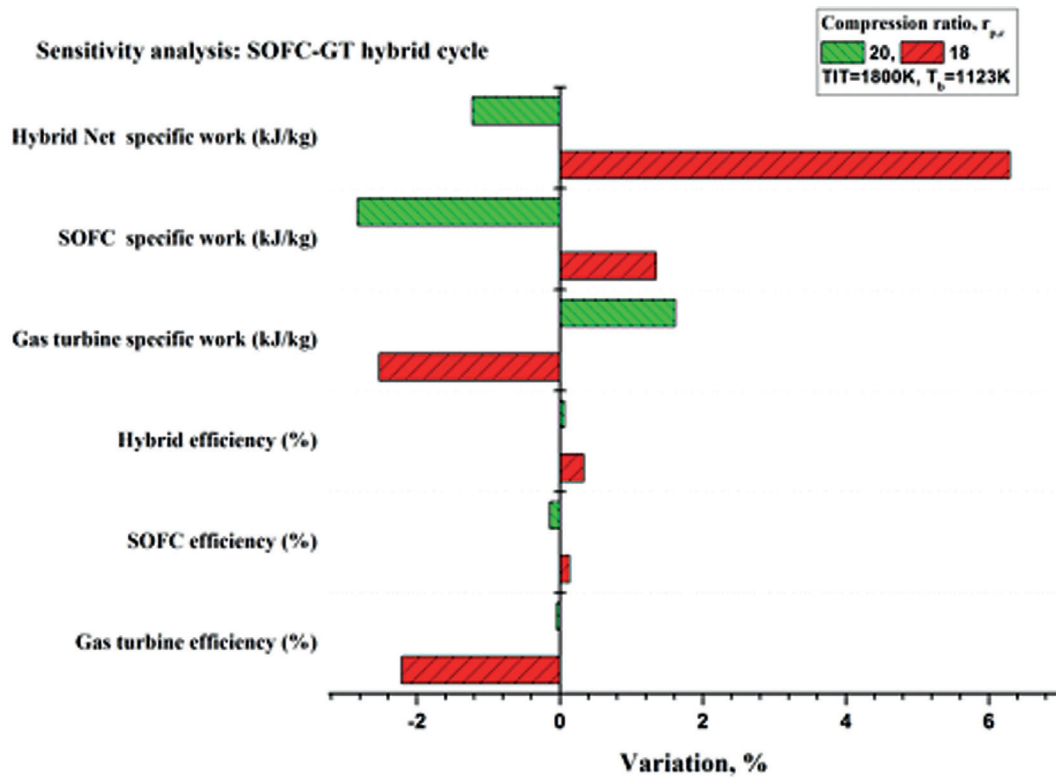


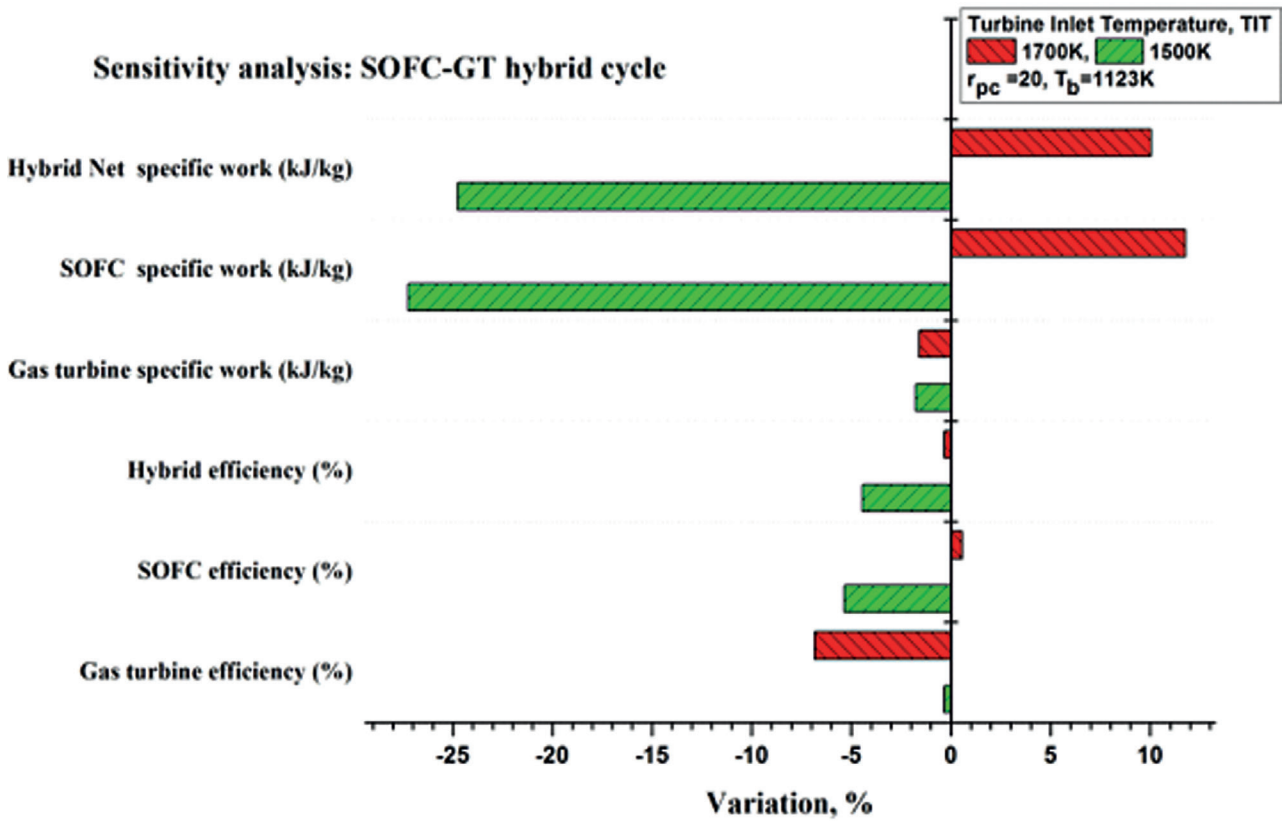
Figure 4. Variation of turbine inlet temperature w.r.t to mass of blade coolant.

Fig. 5(b) illustrates the sensitivity analysis of SOFC-GT hybrid cycle. For sensitivity analysis, TIT 1600K has been considered as a baseline. The influence of change in turbine inlet temperature (TIT) on thermodynamic performance has been analyzed. The result shows that for a decrease in TIT from 1600K to 1500K, there is a decrease in hybrid efficiency, gas turbine efficiency, and SOFC efficiency by 4.43%, 0.335%, and 5.34%, respectively. The noteworthy

decline in the performance of hybrid efficiency and SOFC is there because the recuperation level directly depends upon the turbine outlet temperature. If the TIT gets reduced, it ultimately affects the SOFC performance through recuperation. This can be more evident when TIT increases from 1600K to 1700K, SOFC efficiency, SOFC specific work, and hybrid Net specific work increases by 0.55%, 11.76%, and 10.04%, respectively.



(a) variation of compression ratio



(b) variation of turbine inlet temperature

Figure 5. Sensitivity analysis.

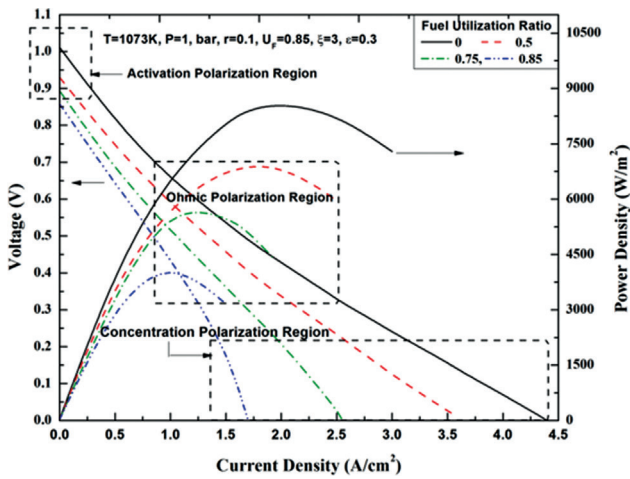


Figure 6. Effect of fuel utilization ratio on fuel cell performance.

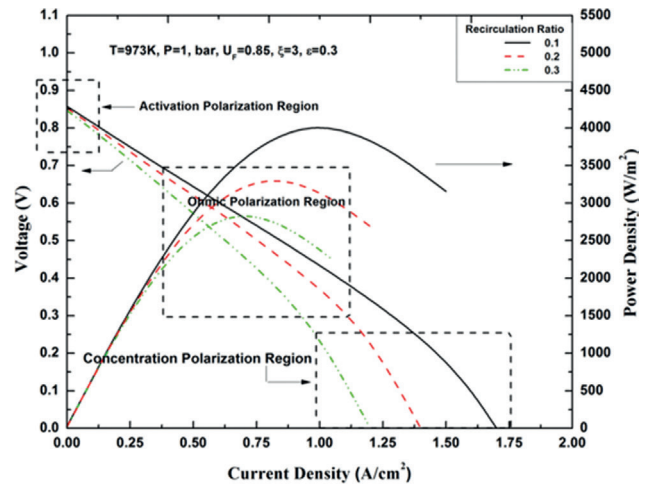


Figure 7. Effect of recirculation ratio on fuel cell performance.

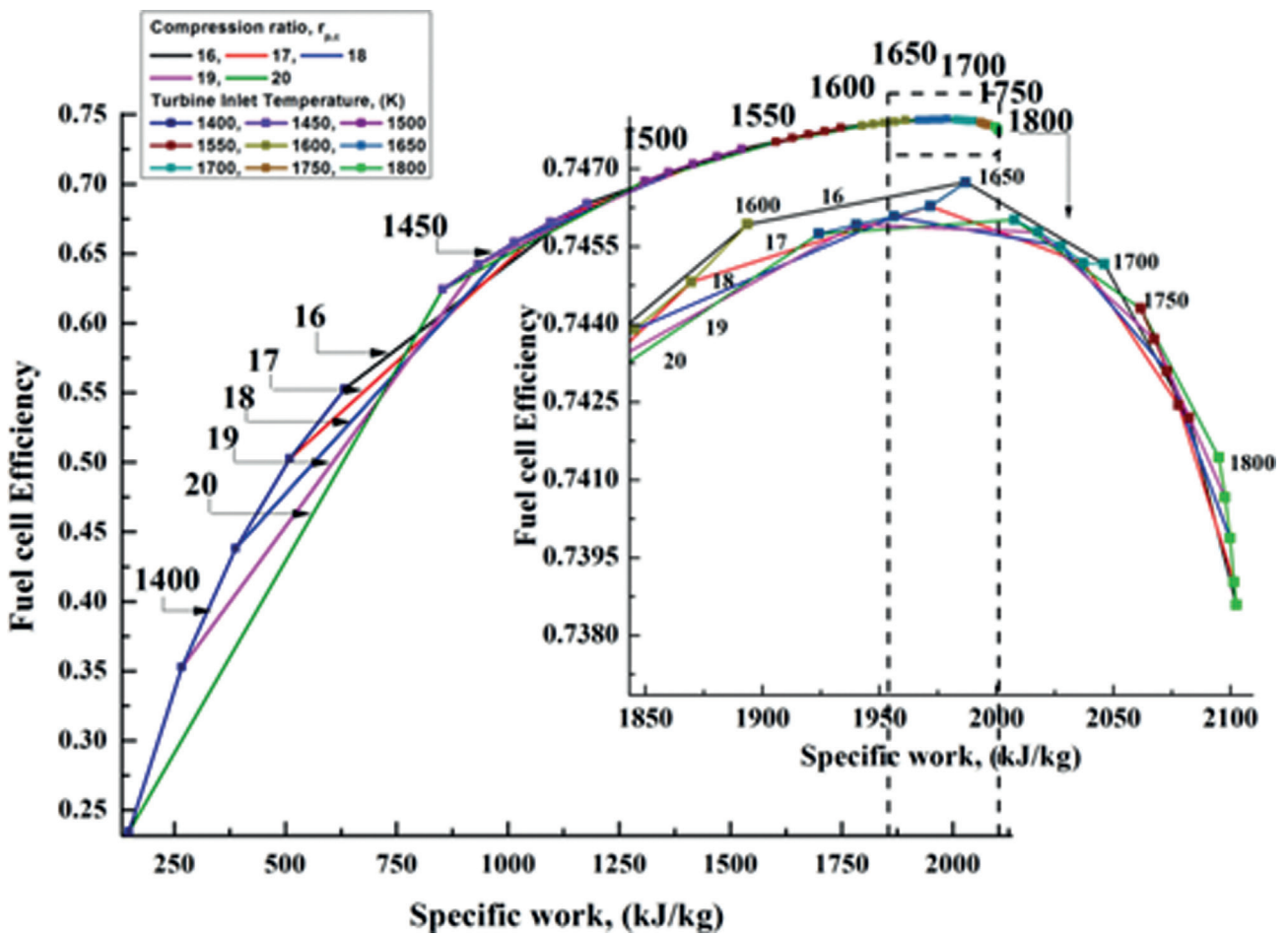


Figure 8. Fuel cell performance map.

Fig. 6 shows the pattern of fuel cell voltage and power at different fuel utilization ratio values. It can be observed that on increased fuel utilization ratio, the power density and voltage eventually decrease due to the existence of a high degree of activation polarization across the anode area. However, the ohmic polarization in the cathode region remains negligible. Therefore, fuel composition plays a major role in fuel cell performance as various fuels undergo various electrochemical reactions, as they have distinct activation polarization.

Recirculation of fuel and air is carried out to ensure a uniform distribution of the temperature inside the fuel cell. The performance curves of voltage and power density at various values of recirculation ratio is illustrated in fig. 7. It has been found that the performance of fuel cell declines as the recirculation ratio enhances. This is due to a significant decrease in the molar concentration of  $H_2$  and  $CO$  through

the fuel channel. Using recirculation, the uniform temperature within the fuel cell can be achieved, but on the other hand, recirculation dilutes the fuel stream, which lowers the performance of fuel cell.

**Performance Map**

An exclusive performance map has been plotted from the parametric analysis for fuel cell and hybrid cycle, as shown in fig.8 and 9. Fuel cell performance and the efficiency of the hybrid plant can be seen by rising as the compression ratio and TIT to an acceptable level and decreases further on the increase in compression ratio and TIT. This is due to an improvement in the degree of recuperation, improving fuel cell efficiency as fuel cell polarization decreases.

It can also be seen from the graph that the trend in the efficiency of hybrid plants and the specific work is the

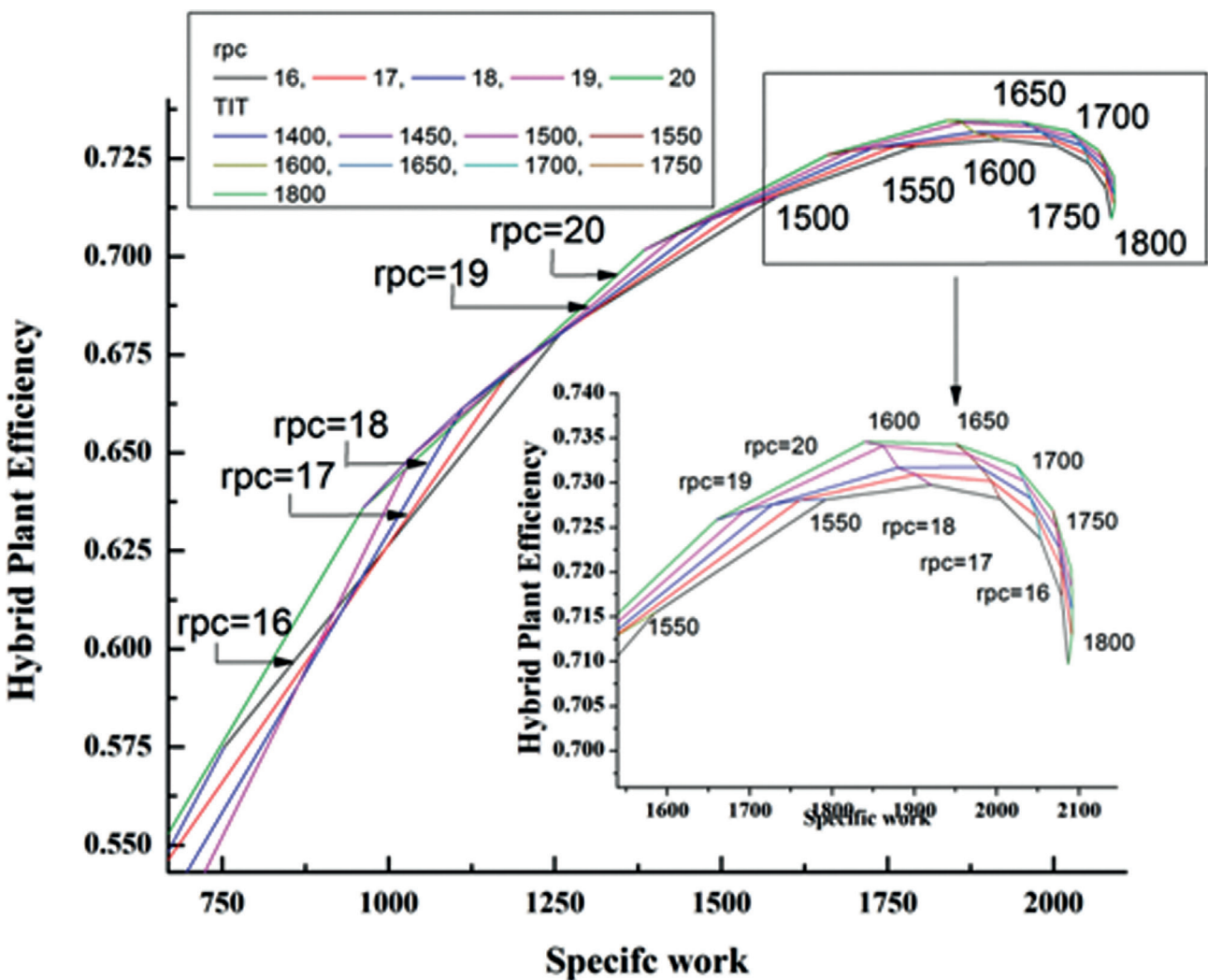


Figure 9. SOFC-GT hybrid cycle performance map.

combined effect of gas turbines and fuel cells. The trend is similar to the fuel cell performance map, as the fuel cell is the major power producer as compared to the gas turbine.

Based on Fig.8, maximum fuel cell efficiency of (about 74.65%) occurred at TIT 1700K and  $r_{pc}=20$ . Similarly, from Fig. 9 maximum efficiency of 73.42% has been achieved for the SOFC-GT hybrid cycle at  $r_{pc}=20$  and TIT=1600K.

### CONCLUSION

In this article, a recuperated blade cooled gas turbine has successfully integrated with high temperature internal reformed SOFC. Apply thermodynamic 1<sup>st</sup> law, thermodynamic analysis has been carried out, and a MATLAB program has been developed. Several conclusions were drawn based on the results obtained.

- From sensitivity analysis, the performance of the hybrid cycle is more sensitive towards TIT as compared to the compression ratio. For instance, on increasing TIT from 1600K to 1700K, SOFC specific work and hybrid Net specific work increase by 11.76% and 10.04%.
- The mass of the blade coolant increases with a higher TIT and compression ratio. However, the TIT variation is noteworthy.
- The efficiency of the fuel cell decreases as the recirculation ratio increases. Whereas, increase in TIT, increases the degree of recuperation, improves the efficiency of a fuel cell.
- The maximum hybrid output of 73.42 percent was at  $r_{pc}=20$  and TIT=1600K
- Based on the parametric thermodynamic analysis, a novel efficiency map gas plotted for fuel cell and hybrid cycle.

The result presented for the proposed hybrid cycle opens a new research line for the researchers and power plant designers whose work focuses on developing alternative energy conversion technologies. Consequently, this would assist them in developing a more feasible integration option for the SOFC-GT hybrid power cycle.

### NOMENCLATURE

A	Active surface area, cm <sup>2</sup>
Da <sub>eff</sub>	Effective gaseous diffusivity through the anode, cm <sup>2</sup> /s
Dc <sub>eff</sub>	Effective gaseous diffusivity through the cathode, cm <sup>2</sup> /s
E	Voltage, V
F	Faraday constant, C
h	Enthalpy, kJ/kg
$\bar{h}$	Specific molar enthalpy, J/mol
H	Enthalpy flow rate, W
icd <sub>a</sub>	Exchange current density of anode, A/cm <sup>2</sup>

i	Current density, A/cm <sup>2</sup>
icd <sub>c</sub>	Exchange current density of cathode, A/cm <sup>2</sup>
ias	Anode-limiting current density, A/cm <sup>2</sup>
ics	Cathode-limiting current density, A/cm <sup>2</sup>
I	Current, A
K	Equilibrium constant
s	Entropy
T	Thickness of a cell component, $\mu$ m
LHV	Lower heating value, J/mol
$\dot{m}$	Mass flow rate, kg/s
M	Molecular weight, g/mol
$n_e$	Number of Electrons
r	Recirculation ratio
P	Pressure, bar
R	Universal gas constant, J/molK
T	Temperature, K
TIT	Turbine inlet temperature, K
$U_F$	Fuel Utilization ratio
$U_a$	Air Utilization ratio
$W_{fc}$	Power output of cell, W
$\dot{W}$	Power, kW
X	Molar Concentration

### Greek Letter

$\emptyset$	Thermodynamic property function
$\epsilon$	Effectiveness
$\rho_k$	Electrical resistivity of the cell components
$\eta$	Cell Efficiency
$\Delta\bar{G}$	Change in specific molar gibbs free energy j/mol

### Subscripts

a	air/ambient
an	Anode
act	Activation
b	blade
c	Coolant
cat	Cathode
ch	channel
conc	Concentration
comb	Combustor
comp	Compressor
elec	Electrolyte
f	Fuel
fc	Fuel cell
g	Gas
e	Exit
in	inlet
j	Coolant stream
k	components
net	Difference
ohm	Ohmic
w	Water
rc	Recuperator

## Acronyms

AEI	Anode Electrolyte Interface
GT	Gas Turbine
PEN	Positive Electrode/ Electrolyte/Negative-Electrode
SOFC	Solid Oxide Fuel Cell
TIT	Turbine Inlet Temperature

## AUTHORSHIP CONTRIBUTIONS

Authors equally contributed to this work.

## DATA AVAILABILITY STATEMENT

The authors confirm that the data that supports the findings of this study are available within the article. Raw data that support the finding of this study are available from the corresponding author, upon reasonable request.

## CONFLICT OF INTEREST

The author declared no potential conflicts of interest with respect to the research, authorship, and/or publication of this article.

## ETHICS

There are no ethical issues with the publication of this manuscript.

## REFERENCES

- [1] Duic N, Guzovic Z, Kafaroklemes JJ, Mathiessen BV, Yin J. Sustainable development energy, water and environment systems. Afgan NH, Bogdan Z, Duić N, Guzović Z, editors. Proceedings of the 3rd Dubrovnik Conference; 2005 Jun 5-10; Dubrovnik, Croatia: Nova Scientific; 2005. pp. 3–5.
- [2] Massardo AF, Lubelli, F. Internal reforming solid oxide fuel cell-gas turbine combined cycles (IRSOFC-GT): Part A – cell model and cycle thermodynamic analysis. *J Eng Gas Turbines Power* 2000;122:27–35. [\[CrossRef\]](#)
- [3] Hirschenhofer JH, Stauer DB, Engleman RR, Klett MG. *Fuel Cell Handbook*. 4th ed. Los Angeles: Parsons Corporation; 1998. [\[CrossRef\]](#)
- [4] Möller BF, Arriagada J, Assadi M, Potts I. Optimisation of an SOFC/GT system with CO<sub>2</sub>-capture. *J Power Sources* 2004;131:320–326. [\[CrossRef\]](#)
- [5] Song TW, Sohn JL, Kim TS, Ro ST. Performance characteristics of a MW-class SOFC/GT hybrid system based on a commercially available gas turbine. *J Power Sources* 2006;158:361–367. [\[CrossRef\]](#)
- [6] Akkaya AV, Sahin B, Erdem HH. An analysis of SOFC/GT CHP system based on exergetic performance criteria. *Int J Hydrog Energy* 2008;33:2566–2577. [\[CrossRef\]](#)
- [7] Kandepu R, Imsland L, Foss BA, Stiller C, Bolland O, Thorud B. Modeling and control of a SOFC-GT-based autonomous power system. *Energy* 2007;32:406–417. [\[CrossRef\]](#)
- [8] Santin M, Traverso A, Magistri L, Massardo A. Thermoeconomic analysis of SOFC-GT hybrid systems fed by liquid fuels. *Energy* 2010;35:1077–1083. [\[CrossRef\]](#)
- [9] Thomas AA, Barton PI. Combining coal gasification, natural gas reforming, and solid oxide fuel cells for efficient polygeneration with CO<sub>2</sub> capture and sequestration. *Fuel Process Technol* 2011;92:2105–2115. [\[CrossRef\]](#)
- [10] Gholamian E, Zare V. A comparative thermodynamic investigation with environmental analysis of SOFC waste heat to power conversion employing Kalina and Organic Rankine Cycles. *Energy Convers Manag* 2016;117:150–161. [\[CrossRef\]](#)
- [11] Aminyavari M, Mamaghani AH, Shirazi A, Najafi B, Rinaldi F. Exergetic, economic, and environmental evaluations and multi-objective optimization of an internal-reforming SOFC-gas turbine cycle coupled with a Rankine cycle. *Appl Therm Eng* 2016;108:833–846. [\[CrossRef\]](#)
- [12] Rokni M. Thermodynamic analysis of SOFC (solid oxide fuel cell)–Stirling hybrid plants using alternative fuels *Energy* 2013;61:87–97. [\[CrossRef\]](#)
- [13] Zhao H, Jiang T, Hou H. Performance analysis of the SOFC–CCHP system based on H<sub>2</sub>O/Li–Br absorption refrigeration cycle fueled by coke oven gas. *Energy* 2015;91:983–993. [\[CrossRef\]](#)
- [14] Chitsaz A, Mehr AS, Mahmoudi SMS. Exergoeconomic analysis of a trigeneration system driven by a solid oxide fuel cell, *Energy Convers Manag* 2015;106:921–931. [\[CrossRef\]](#)
- [15] Choudhary T, Sahu M, Krishna S. Thermodynamic analysis of solid oxide fuel cell gas turbine hybrid system for aircraft power generation. *SAE Technical Paper* 2017-01-2062. [\[CrossRef\]](#)
- [16] Siddiqui O, Dincer I. Analysis and performance assessment of a new solar-based multi-generation system integrated with ammonia fuel cell and solid oxide fuel cell-gas turbine combined cycle. *J Power Sources* 2017;370:138–154. [\[CrossRef\]](#)
- [17] Choudhary T, Sanjay. Computational analysis of IR-SOFC: Thermodynamic, electrochemical process and flow configuration dependency. *Int J Hydrog Energy* 2016;41:1259–1271. [\[CrossRef\]](#)
- [18] Choudhary T, Sanjay. Computational analysis of IR-SOFC: Transient, thermal stress, carbon deposition and flow dependency. *Int J Hydrog Energy* 2016;41:10212–10227. [\[CrossRef\]](#)

- [19] Choudhary T, Sahu MK, Sanjay. CFD modeling of SOFC Cogeneration system for building application. *Energy Procedia* 2017;109:361–368. [\[CrossRef\]](#)
- [20] Corigliano O, Fragiaco P. Numerical modeling of an indirect internal CO<sub>2</sub> reforming solid oxide fuel cell energy system fed by biogas. *Fuel* 2017;196:352–361. [\[CrossRef\]](#)
- [21] Peksen M, Al-Masri A, Peters R, Blum L, Stolten D. Recent developments in 3D multiphysics modelling of whole fuel cell systems for assisting commercialisation and improved reliability. *ECS Trans* 2017;75:15–22. [\[CrossRef\]](#)
- [22] He Z, Li H, Birgersson KE. Full Three-Dimensional Modelling of PEMFC and Planar SOFC. *Reduced modelling of planar fuel cells*. 1st ed. Berlin: Springer; 2017. p. 55–87. [\[CrossRef\]](#)
- [23] Sanjay, Singh O, Prasad BN. Comparative performance analysis of cogeneration gas turbine cycle for different blade cooling means. *Int J Therm Sci* 2009;48:1432–1440. [\[CrossRef\]](#)
- [24] Choudhary T, Kumari A, Sanjay R, Mohapatra A, Kumar Sahu M. Thermodynamic modeling of blade cooled turboprop engine integrated to solid oxide fuel cell: A concept. *SAE Technical Paper* 2018-01-1308. [\[CrossRef\]](#)
- [25] Kumari A, Choudhary T, Sanjay Y, Murty P, Sahu M. Thermodynamic and emission analysis of basic and intercooled gas turbine cycles. *SAE Technical Paper* 2015-01-2426. [\[CrossRef\]](#)
- [26] Choudhary T, Sanjay. Thermodynamic assessment of SOFC- ICGT hybrid cycle: Energy analysis and entropy generation minimization. *Energy* 2017;134:1013–1028. [\[CrossRef\]](#)
- [27] Choudhary T, Sanjay Y, Murty P. Parametric analysis of syn-gas fueled sofc with internal reforming. *SAE Technical Paper* 2015-01-1176. [\[CrossRef\]](#)
- [28] Zhao H, Zhao Z, Wang H. Thermodynamic performance study of the CLHG/SOFC combined cycle system with CO<sub>2</sub> recovery. *Energy Convers Manag* 2020;223:113319. [\[CrossRef\]](#)
- [29] Sezer H, Mason JH, Celik IB, Yang T. Three-dimensional modeling of performance degradation of planar SOFC with phosphine exposure. *Int J Hydrog Energy* 2021;46:6803–6816. [\[CrossRef\]](#)
- [30] Akroot A, Namli L, Ozcan H. Compared Thermal modeling of anode- and electrolyte-supported SOFC-gas turbine hybrid systems. *J Electrochem En Conv Stor* 2021;18:011001. [\[CrossRef\]](#)
- [31] Guo F, Qin J, Ji Z, Liu H, Cheng K, Zhang S. Performance analysis of a turbo-fan engine integrated with solid oxide fuel cells based on Al-H<sub>2</sub>O hydrogen production for more electric long-endurance UAVs. *Energy Convers Manag* 2021;235:13999. [\[CrossRef\]](#)